IMAGE QUALITY MEASURE USING CURVATURE SIMILARITY

Susu Yao, W. Lin, Z.K Lu, E.P. Ong, M.H. Locke and S.Q. Wu

Institute for Infocomm Research, Singapore 119613
E-mail: ssyao@i2r.a-star.edu.sg

ABSTRACT

This paper proposes a new full-reference objective metric for image quality assessment. The reference and distorted images are decomposed into a number of wavelet subbands, in which mean curvatures and perceived error of the wavelet coefficients of two images are computed and integrated to give overall quality index. Taking structural similarity and error visibility into account, the new method can achieve high consistency with subjective evaluation compared with other metrics. Experimental results have shown the effectiveness of the proposed metric.

Index Terms— Image quality assessment, surface curvature, correlation, wavelet transform, error visibility.

1. INTRODUCTION

The quality of a digital image is affected by many factors. In practical image processing such as acquisition, compression, transmission and reconstruction, the visual quality of image is degraded in different degrees due to added noise or loss of image information. Usually, we compare original image and processed image to evaluate visual quality, namely full-reference quality assessment. Subjective evaluation is most accurate but it is time-consuming and inconvenient. Objective evaluation methods which can automatically predicate perceived visual quality are desirable in most practical image processing systems such as image and video coding, dynamic monitoring of image quality. A number of objective image quality assessment methods have been proposed in past few years [1,2,3], in which many efforts have gone into the investigation of error sensitivity in spatial or frequency domain. However, psychological experiments have revealed that the human visual system (HVS) has more sensitivity to the structural information variation than to the error visibility. Obvious evidence is that human eyes are less sensitive to the small mean value shift of an image than to the distortions at image discontinuities. Based on this fact, Wang [4] proposed an image quality assessment method in which one of three factors measures the structural similarity using vector correlation. However, the spatial vector correlation cannot distinguish effectively the structural variation. This paper attempts to further exploit structural similarity in wavelet bands using differential geometric information because human eyes are able to deal with many geometric deformations quickly and accurately. In 3-D space, a surface model can represent image regions including flat surfaces, piecewise-smooth curved surfaces, edges and texture. We use surface curvature similarity between reference and distorted images as a factor to measure quality degradation. On the other hand, the frequency sensitivity of human perception for the wavelet coefficients is also taken into account to compute perceived errors that are integrated with the measure of curvature similarity to give overall image quality index. The effectiveness of the proposed method is verified through evaluating an image test database. The experimental results show that the new method can give a high correlation with the subjective scores in terms of prediction accuracy, monotonicity and consistence.

This paper is organized as follows. In Section 2, wavelet decomposition and error sensitivity of wavelet coefficients are described. Section 3 gives brief description of surface curvature. Section 4 presents the proposed image quality assessment method. Experimental results and comparison with other metrics are given in Section 5. Finally, conclusions are drawn in Section 6.

2. WAVELETS AND ERROR SENSITIVITY MODEL

2.1. Wavelet Decomposition

The wavelet transform is one of the most powerful techniques for image processing because of its similarities to the multiple channel models of the HVS. In recent years, image quality measures have used wavelet transform to perform spatial frequency decomposition [6][7].

Figure 1 shows a two-dimensional frequency space in which four-level hierarchical wavelet subbands are obtained using DWT 9/7 biorthogonal filters. In this space, there are total 13 subbands with one low-frequency subband and 12 AC subbands. Each level in the decomposition contains an LH band, an HL band, and an HH band.

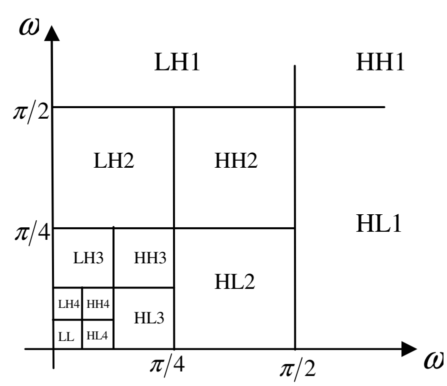

Figure 1. Titling of the two-dimensional frequency space by four-level hierarchical wavelet decomposition.

2.2. Wavelet Frequency Error Sensitivity Model

It has been found that human eyes have different sensitivities to the different frequency bands. In [5], the base detection thresholds for the 9/7 DWT are measured using a noise added to the wavelet coefficients of a blank image of grey level 128. By fitting the data from the psychophysical experimental results in a mathematical model for a visually detectable noise threshold *y*, which is written as follows:

$$\log y = \log a + k(\log f - \log g_\theta f_0)^2 \tag{1}$$

where, θ is the orientation of wavelet subband ($\theta = HH, HL, LH$), f the spatial frequency (cycles/degree) determined by both the display resolution r, viewing distance and wavelet decomposition level λ. $f = r2^{-\lambda}$. a, k, f_0 and g_θ are constants which can be found in [5]. The wavelet error detection threshold is then given by

$$WT_{\lambda,\theta} = \frac{a}{A_{\lambda,\theta}} 10^{k\left(\log\left(2^{\lambda} f_0 g_\theta / r\right)^2\right)} \tag{2}$$

Where, $A_{\lambda,\theta}$ is the amplitude of the DWT 9/7 basis function corresponding to level λ and orientation θ.

It is easy to verify from the equation (2) that the threshold for HH band is the highest while the threshold for LL band is the lowest. In other words, human eyes are more sensitive to the low frequency band than to the high frequency band. They are also dependent on orientation, being most sensitive in the horizontal and vertical directions and least sensitive at oblique angles.

Taking into account of the masking effect [7], which is a function of the actual values of the wavelet coefficients, the detection threshold will elevate, which can be given by:

$$T_{\lambda,\theta}(u,v) = \max\left(WT_{\lambda,\theta}, C_{\lambda,\theta}(u,v)\right) \tag{3}$$

Where, $C_{\lambda,\theta}(u,v)$ denotes the wavelet coefficients and (u,v) the coordinate. Due to elevated detection threshold the perceived error between the wavelet coefficients of original and distorted images denoted as $C^o_{\lambda,\theta}(u,v)$ and $C^d_{\lambda,\theta}(u,v)$ will be reduced, which can be written as follows:

$$\Delta C_{\lambda,\theta}(u,v) = \left(C^o_{\lambda,\theta}(u,v) - C^d_{\lambda,\theta}(u,v)\right) / T_{\lambda,\theta}(u,v) \tag{4}$$

3. SURFACE CURVATURE

A two-dimensional surface model can represent an image with smooth, edge and texture regions. We assume that the surface of an image can be specified as the height $I(u,v)$ above the support plane defined by two coordinates (u,v). A 3-D point on the surface is given by $z(u,v) = (u, v, I(u,v))$. Let *p* be a point on the surface *S*. Consider all curves on *S* passing through the point *p* on the surface. Every such curve c_i has an associated curvature K_i, among them the maximal and minimal values are known as the principal curvatures of the surface, which are denoted as $\kappa_{\max}$ and $\kappa_{\min}$. The product of $\kappa_{\max}$ and $\kappa_{\min}$ is called Gaussian curvature at $p \in S$, i.e., $K = \kappa_{\max} \cdot \kappa_{\min}$. The corresponding average is known as the mean curvature at $p \in S$, $H = (\kappa_{\max} + \kappa_{\min})/2$ [8]. The mean curvature H of a surface *S* is a measure of curvature that comes from differential geometry and that locally describes the curvature of an embedded surface.

These two curvatures are given by:

$$H = \frac{I_{uu} + I_{vv} + I_{uu} I_v^2 + I_{vv} I_u^2 - 2 I_u I_v I_{uv}}{2\left(1 + I_u^2 + I_v^2\right)^{\frac{3}{2}}} \tag{5}$$

$$K = \frac{I_{uu} I_{vv} - I_{uv}^2}{\left(1 + I_u^2 + I_v^2\right)^2} \tag{6}$$

Where, I_u, I_v, I_{uu}, I_{uv} and I_{vv} are the partial derivatives of I.

Surface curvature is complementary to edge information, which is a useful feature for scene analysis, feature extraction, and object recognition. It has been widely used for image segmentation and classification in computer vision. In image coding, visual quality is usually affected by the appearance of coding artifacts, such as blockiness, blurring and ringing effects. These coding artifacts deform the surface structure information and cause perceived noisiness. As an example, Fig. 2 shows the original and coded images with their curvature maps, from which we can see that the curvatures of distorted image at smooth regions such as face and background are quite different from original curvature at those points. Therefore by computing curvature similarity between two images can measure the degradation degree of the image quality.

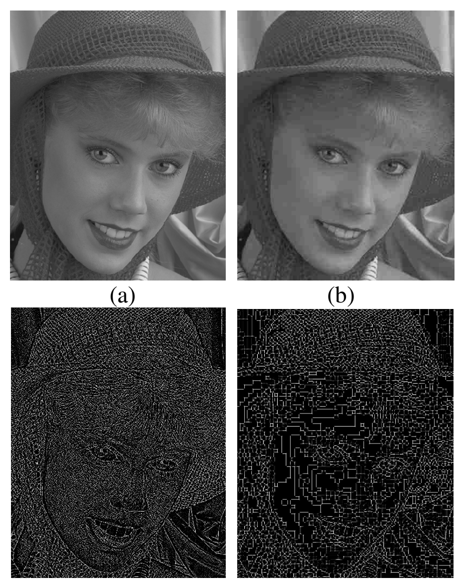

(a) (b) (c) (d)

Fig. 2. (a) Original image; (b) JPEG coded image; (c) Mean curvature map of (a); (d) Mean curvature map of (b)

4. THE PROPOSED IMAGE QUALITY METRIC

In this section, a full-reference image quality metric is presented. Firstly, the reference image and its distorted version are decomposed into four-level structure with total 13 subbands using 9/7 biorthogonal wavelet filter banks. In each subband, mean surface curvature maps are obtained using equation (5). The similarity between two images can be quantified in terms of the correlation function. We calculate the correlation coefficients between two curvature maps of original and distorted images in the wavelet subbands using following formula:

$$Corr\left(H^o, H^d\right) = \frac{\sum_{u,v}\left(H^o_{u,v} - \mu_o\right)\left(H^d_{u,v} - \mu_d\right)}{\sqrt{\sum_{u,v}\left(H^o_{u,v} - \mu_o\right)^2 \sum_{u,v}\left(H^d_{u,v} - \mu_d\right)^2}} \quad (7)$$

Where, $H^o_{u,v}$ and $H^d_{u,v}$ denote mean curvatures of original image and its distorted image at point (u,v) on the surface, respectively. μ_o and μ_d are the corresponding mean values of $H^o_{u,v}$ and $H^d_{u,v}$.

Taking perceived error of wavelet coefficients and structural similarity into account, the overall quality measure using curvature similarity, namely QMCS in short, is obtained by summing the values of quality index in all the subbands, which is written as follows:

$$QMCS = \sum_{\lambda,\theta}\left(\frac{1}{1 + \frac{\left|Corr\left(H^o_{\lambda,\theta}, H^d_{\lambda,\theta}\right)\right|^{0.5}}{\sqrt{\frac{1}{N_{\lambda,\theta}}\sum_{u,v}\left(\Delta C_{\lambda,\theta}(u,v) - \mu_{\Delta C_{\lambda,\theta}}\right)^2}}}\right) \quad (8)$$

Where, $\mu_{\Delta C_{\lambda,\theta}}$ denotes the mean value of $\Delta C_{\lambda,\theta}(u,v)$, $\lambda = 1,\cdots,4$, and $N_{\lambda,\theta}$ is the number of pixels at level λ and orientation θ. With this equation, we can obtain a quality score for each image. As the difference between two images tends towards zero $\Delta C_{\lambda,\theta} \to 0$, the correlation coefficient tends towards 1, the quality score approaches zero.

5. EXPERIMENTAL RESULTS

5.1. The Test Image Database

We use the image database [10] developed by the Laboratory of Image and Video Engineering (LIVE), the University of Texas at Austin to test the performance of the proposed quality metric. The database is composed of total 344 images that were obtained by compressing twenty-nine high-resolution 24-bits/pixel RGB color images, including 175 JPEG compressed images and 169 JPEG 2000 compressed images. The compression bit rates were in the range of 0.150 to 3.336 and 0.028 to 3.150 bits/pixel, respectively.

In subjective evaluation procedure, observers are asked to provide their votes of perceived image quality on a continuous linear scale that was divided into five-grade description marked with “Bad”, “Poor”, “Fair”, “Good” and “Excellent”. Each JPEG and JPEG 2000 compressed image was viewed by 13~20 subjects and 25 subjects, respectively. The raw scores given by each subject were scaled to the full range (1~100). Finally, subjective Mean Opinion Score (MOS) value for each distorted image is obtained by taking the average of those rating values.

5.2. Criteria for Metric Performance

Following the performance evaluation methods adopted in the VQEG Phase-I test [9], we use three evaluation criteria to give quantitative measures on the performance of the proposed method. The first criterion is called non-linear correlation, which measures the prediction accuracy, i.e., the ability of a metric to predict subjective ratings. It is given by computing the normalized correlation coefficient between subjective MOS and objective rating that is fitted via a four-parameter cubic polynomial to the corresponding MOS, called non-linear regression analysis. The second criterion is the Spearman rank-order correlation, which measures the prediction monotonicity of a model, i.e., whether the increases or decreases in one variable are associated with the variation of other variable. The third one is outlier ratio, which calculates the percentage of the number of predictions outside the range of ± 2 times of the standard deviations, which is used as a measure of prediction consistency. Besides, we also use Mean Absolute Error (MAE) and Root Mean Square Error (RMSE) as the performance indexes for the purpose of comparison with other quality assessment metrics.

5.3. Experimental Results and Performance Comparison

For each image in the database, we compute its objective quality score using the proposed method. Then performance indexes including non-linear correlation, Spearman rank-order correlation, outlier ratio, MAE and RMSE are calculated. In order to compare the proposed quality metric with other competitive metrics on the same database, three main quality assessment methods have been tested, which are named PSNR, Sarnoff [11], MSSIM [4]. The experimental results are listed in Table I. Figs. 3-6 draw the scatter plots of MOS versus PSNR, Sarnoff, MSSIM and proposed QMCS, respectively. From the experimental results, we can see that a significant improvement for the image quality measure in terms of five performance evaluation indexes has been achieved in comparison with MSSIM method that used spatial vector correlation as the measure of structural information. It should be pointed out that the data in Table I and scatter plots (Figs.3-5) for PSNR, Sarnoff, and MSSIM models are from [4] for the purpose of comparison.

Table I. Performance comparison of image quality assessment models; PCC: correlation coefficient; MAE: mean absolute error; RMSE: root-mean-square error; OR: outlier ratio; SROCC: spearman rank-order correlation coefficient

	Non-linear Regression				Rank-order
Model	PCC	MAE	RMSE	OR	SROCC
PSNR	0.905	6.53	8.45	0.157	0.901
Sarnoff	0.956	4.66	5.81	0.064	0.947
MSSIM	0.967	3.95	5.06	0.041	0.963
QMCS	0.971	3.81	4.75	0.012	0.966

6. CONCLUSIONS

In this paper, we have presented a new method for image quality evaluation. From the view point of comparing structural information variation of a reference image and distorted image, we used mean curvature similarity combined with perceived error of the wavelet coefficients. Experiments on JPEG and JPEG 2000 compressed image database have shown that the new quality metric can obtain a high correlation with subjective evaluation scores in terms of prediction accuracy, monotonicity and consistency.

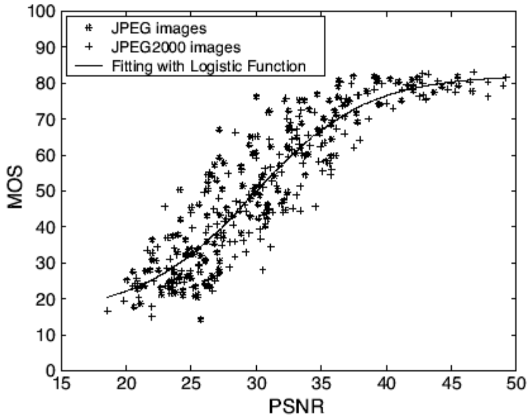

Fig. 3. Scatter plot of MOS vs. PSNR

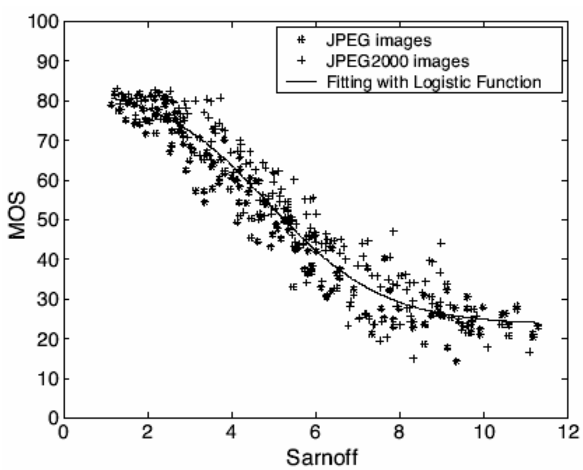

Fig.4. Scatter plot of MOS vs. Sarnoff

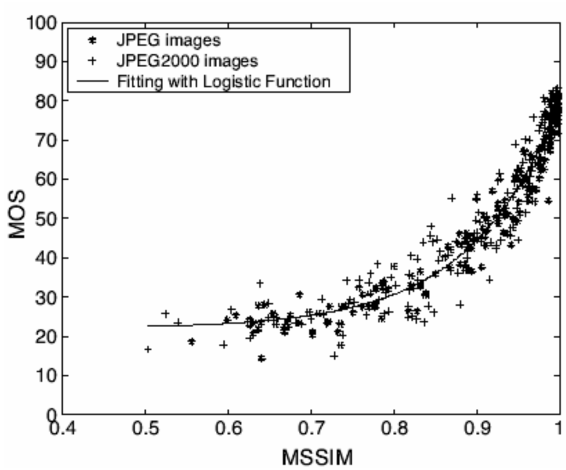

Fig.5. Scatter plot of MOS vs. MSSIM

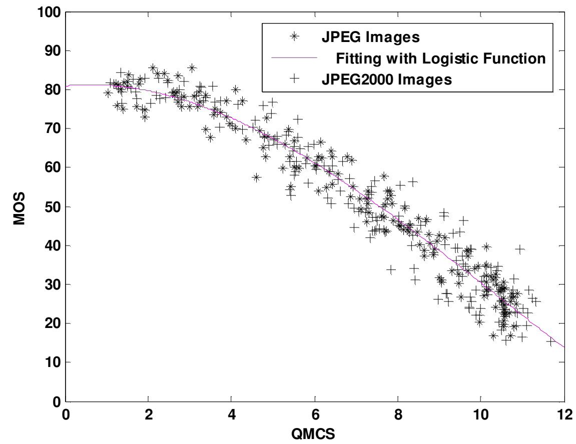

Fig. 6. Scatter plot of MOS vs. QMCS

REFERENCES

[1] S. Winkler, "Quality metric design: a closer look", *Proceedings of the SPIE Human Vision and Electronic Imaging*, vol. 3959, pp.37-44, San Jose, CA, Jan. 22-28, 2000.

[2] Z. Yu, H.R. Wu, S. Winkler, T. Chen, "Vision model based impairment metric to evaluate blocking artifacts in digital video", *Proceedings of IEEE*, Vol.90, No.1, pp.154-169, 2002.

[3] P.C. Teo and D.J. Heeger, "Perceptual image distortion," *Proc. SPIE*, vol. 2179, pp.127-141, 1994.

[4] Z. Wang, et.al., "Image quality assessment: from error visibility to structural similarity", IEEE *Trans. Image Processing*, vol.13, No.4, pp. 600-612, 2004.

[5] A.B. Watson, G.Y. Yang, J.A. Solomon, and J. Villasenor, "Visibility of wavelet quantization noise," *IEEE Trans. Image Processing*, Vol. 6, No. 8, pp. 1164-1175, 1997.

[6] Y.K. Lai and C.-C. J. Kuo, "A Haar wavelet approach to compressed image quality measurement," *J. Vis. Commun. Image Represent.*, Vol. 11, pp.17-40, 2000.

[7] A.P. Bradley, "A wavelet visible difference predictor," *IEEE Trans. Image Processing,* Vol. 8, pp. 717-730, May 1999.

[8] M.do Carmo, "Differential geometry of curves and surface," Prentice-Hall, 1976.

[9] VQEG: The Video Quality Expertise Group, http://www.vqeg.org/.

[10] H.R. Sheikh, Z. Wang, L. Cormack, and A.C. Bovik, "LIVE image quality assessment database", http://live.eve.utexas.edu/research/quality (2003).

[11] Sarnoff Corporation, "JNDmetrix Technology," http://www.sarnoff.com/products_services/video_vision/jndmetrix/.